Macroporous Chelating Resins Incorporating Heterocyclic Functional Groups via Hydrophilic Poly(ethylene oxide) Spacer Arms. II. Adsorption Properties

Chunnuan Ji, Rongjun Qu, Qiang Xu, Changmei Sun, Chunhua Wang, Yucui Cheng, Yanpeng Song

School of Chemistry and Materials Science, Ludong University, Yantai 264025, China

ABSTRACT: Several new chelating resins prepared from macroporous chloromethylated polystyrene-*co*-divinylbenzene by either direct attachment of the heterocyclic functional groups, such as 2-aminopyridine, 2-amino-5-methylthio-1,3,4-thiadizole, 2-amino-5-ethyl-1,3,4-thiadizole, and 2-mercaptobenzothiazole, to the polymeric matrix or through different hydrophilic spacer arms were tested for the adsorption properties toward Hg^{2+}, Ag^{+}, Cd^{2+}, and Pb^{2+} in an ammonium acetate buffer solution of pH 3.0. The results show that these resins exhibited a high affinity for Hg^{2+} and Ag^{+}. The introduction of hydrophilic spacer arms between the polymeric matrix and heterocyclic functional groups resulted in an increase in the hydrophilicity and adsorption capacity of the resins. The presence of spacer arms made the kinetics of adsorption faster. The influence of the length of the spacer arm on the adsorption properties was also investigated. © 2008 Wiley Periodicals, Inc. J Appl Polym Sci 111: 2148–2156, 2009

Key words: adsorption; polystyrene; spacer arm; hetero cyclic functional groups

INTRODUCTION

Chelating resins are materials that are well known for the removal of metal ions from aqueous solutions. Many chelating resins with covalently bonded heterocyclic functional groups containing sulfur and nitrogen atoms [e.g., pyridine,[1–3] 8-hydroxyquinoline,[4,5] benzimidazolylazo[6,7] imidazole,[8,9] pyrazole,[10] 2,5-dimercapto-1,3,4-thiodiazole,[11] and 2-mercaptobenzothiazole (MBZ)[12]] on styrene–divinylbenzene copolymer have been designed for the selective adsorption of heavy- and noble-metal ions. In the aforementioned chelating resins, because the heterocyclic functional groups are directly attached to the polymeric matrix, the nature of the hydrophobicity of the polymer matrix and the heterocyclic functional groups sometimes makes it difficult for the metal ions to diffuse and coordinate with functional groups.[13] As a result, only a fraction of the functional groups in polymers takes part in the coordination with metal ions.

Recently, chelating resins bearing different spacer arms, such as ethylene oxide, ethylene sulfide, and ethylene imine, have been reported.[13–16] It has been found that the presence of spacer arms between the polymeric matrix and functional groups (e.g., thiol, dithiocarbamate, methylthiourea, and triisobutylphosphine) shows remarkable effects on the adsorption kinetics, adsorption capacities, and selectivity of the resins. This effect is ascribed to either an improvement in the hydrophilicity of the functional groups[17,18] or the participation of the spacer arms in the complexation of metal ions.[19,20] Among the aforementioned three kinds of spacer arms, the spacer group of ethylene oxide is more hydrophilic than ethylene imine. So resins containing poly(ethylene oxide) spacers are likely more solvated in aqueous media and exhibit better adsorption capacities than the ones containing poly(ethylene imine). Sanchez et al.[13] reported that when a sulfur atom substitutes oxygen in the spacer

of poly(ethylene oxide), the capacity of the resin is greatly increased.

In a previous article,[21] we reported the synthesis and characterization of new chelating resins incorporating heterocyclic functional groups [e.g., 2-amino-pyridine (AP), 2-amino-5-methylthio-1,3,4-thiadizole (AMTZ), 2-amino-5-ethyl-1,3,4-thiadizole (AETZ), 2-mercaptobenzothiazole (MBZ)] via hydrophilic poly(ethylene glycol) spacer arms with different spacer arms containing ethylene oxide and ethylene sulfide. As a successive work, the aim of this study was to investigate the adsorption capacity of the resins with or without spacer arms for metal ions and the effect of different spacer arms on the water absorption, adsorption kinetics, and distribution coefficient (K_d).

EXPERIMENTAL

Materials

Chloromethylated polystyrene-co-divinylbenzene [PS-Cl; degree of crosslinking = 10%, divinylbenzene = 5.49 mmol/g of Cl, 30–40 mesh, Brunauer–Emmett–Teller (BET) surface area = 31.85 m^2/g, Barret-Joyner-Halenda (BJH) desorption cumulative volume of pores = 0.31 cm^3/g] was purchased from Chemical Factory of Nankai University (Tianjin, China).

The synthesis and characterization of resins **1a–1d** and **2a–2d** containing spacer arms ($SC_2H_4OC_2H_4$ and $SC_2H_4OC_2H_4OC_2H_4$) and heterocyclic groups (AP, AETZ, AMTZ, and MBZ) with PS-Cl as a raw material was described in our previous article in detail.[21] The structures, contents of functional groups, BET surface areas, and so on of resins **1a–1d** and **2a–2d** are listed in Table I.

A stock solution of metal ions (0.1 mol/L) was prepared by the dissolution of an appropriate amount of analytical-grade nitrates in deionized water, respectively. The buffer solutions (pH = 3 and 6) were prepared by the addition of dilute HNO$_3$ to 0.1M ammonium acetate solution.

Instruments and apparatus

Elemental analysis was performed with an Elementar Analysensysteme Gmbh Varioel (Hanau, Germany). The IR spectra were recorded on a Nicolet MAGNA-IR550 (series II) spectrometer (Madison, WI) (test conditions: potassium bromide pellets, 32 scans, resolution = 4 cm^{-1}). The BET surface area and BJH desorption cumulative volume of the pores were determined by the BET and BJH methods, respectively (ASAP-2020 surface area and porosity analyzer). The surface morphology of was examined via scanning electron microscopy (JSF5610LV, Jeol, Tokyo, Japan). The concentration of metal ions was measured via atomic absorption spectroscopy (AAS; GBC-932, Victoria, Australia) according to the cold AAS method. The wavelengths used to determine the concentrations of Cd^{2+}, Pb^{2+}, Hg^{2+}, and Ag$^+$ were 228.8, 271.0, 253.7, and 328.1 nm, respectively. The adjustment of pH was done with a Systronics digital pH meter (Amorim, Portugal). The length of the linear chain and the average end-to-end distance of the resins were calculated on a SGIO2 workstation, with Accelrys Cerious^2 version 4.2, Matsci, software, with the OFFSETUP and POLYMER2 models (conditions: DREIDING 2.21 force field, 300 K, 10,000 steps).

Synthesis of resins a–d

To compare the effect of the spacer arms presented between the polymeric matrix and the heterocyclic functional groups, resins without spacer arms were synthesized. The synthetic route of the resins without spacer arms, along with the resins containing spacer arms ($SC_2H_4OC_2H_4$ and $SC_2H_4OC_2H_4OC_2H_4$) and heterocyclic groups (AP, AMTZ, AETZ, and MBZ), prepared in our previous study[21] is shown in Scheme 1.

Synthesis of resin a

Resin **a** was prepared according to a procedure described in the literature.[1] PS-Cl (1.5 g, ca. 8.23 mmol Cl) was reacted with 2.5 g of AP in 80 mL of dimethylformamide (DMF) at 90°C for 24 h. The reaction mixture was filtered and washed with water. Then, the resin was moved to a Soxhlet extraction apparatus for reflux extraction in 95% ethanol for 4 h and was finally dried *in vacuo* at 50°C for 48 h. The results of the elemental analysis are as follows: C, 75.88%; H, 7.26%; N, 7.90%.

Synthesis of resin b

The reaction involved 1.5 g of PS-Cl, 80 mL of DMF, 3.08 g of AMTZ, and 1.1 g of K$_2$CO$_3$. The procedure for the synthesis and purification of the product was similar to that of resin **a**. The results of the elemental analysis are as follows: C, 67.40%; H, 6.34%; N, 9.18%; S, 13.14%.

Synthesis of resin c

The reaction involved 1.5 g of PS-Cl, 80 mL of DMF, 2.70 g of AETZ, and 1.2 g of K$_2$CO$_3$. The procedure for the synthesis and purification of the product was similar to that of resin **a**. The results of the elemental analysis are as follows: C, 71.21%; H, 6.87%; N, 8.79%; S, 7.40%.

Synthesis of resin d

The reaction involved 1.5 g of PS-Cl, 80 mL of DMF, 3.50 g of MBZ, and 1.1 g of K$_2$CO$_3$. The procedure for the synthesis and purification of the product was similar to that of resin **a**. The results of the elemental

TABLE I
Structures and Contents of the Functional Groups of the Resins

Resin	Structure	BET surface area $(m^2/g)^a$	BJH desorption cumulative volume of pores $(cm^3/g)^a$	c_{fg} of resin $(mmol/g)^b$
a		29.76	0.27	2.83
1a		28.61	0.29	0.64
2a		23.50	0.28	0.25
b		33.95	0.28	2.19
1b		27.37	0.22	0.42
2b		22.00	0.28	0.25
c		27.65	0.25	2.09
1c		29.62	0.19	0.40
2c		24.16	0.28	0.22
d		19.8	0.20	3.17
1d		28.89	0.23	2.18
2d		21.54	0.26	1.51

P denotes the polymer matrix.
[a] The data for the BET surface area and BJH desorption cumulative volume of pores of resins **1a–1d** and **2a–2d** are cited from our previous work.[21]
[b] c_{fg} of the resin was calculated from the nitrogen determined by elemental analysis.

analysis are as follows: C, 69.17%; H, 5.13%; N, 4.44%; S, 20.46%.

Experimental procedure

Water absorption[22]

Water absorption was measured with a centrifugation method, in which approximately 1 g of swollen resin in double-distilled water was placed in a short column with a sintered glass bottom, centrifuged at 5000 rpm for 5 min, weighed, and dried at 80°C overnight. After cooling in a desiccator, the column was reweighed again with and without the resin. To compare the effects of different functional groups on the hydrophilicity of the resins, we introduced the content of functional groups (c_{fg}) into the traditional equation $(m_w - m_d)/m_d$[22] with equation $(m_w - m_d)/(m_d \times c_{fg})$ to calculate the water absorption of each resin, where m_w is the weight of the water-swollen resin after centrifugation and m_d is the dry weight of the resin.

Adsorption kinetics

In the kinetics experiment, 30 mg of the resin was added to a mixture of 19 mL of $0.1M$ acetate buffer
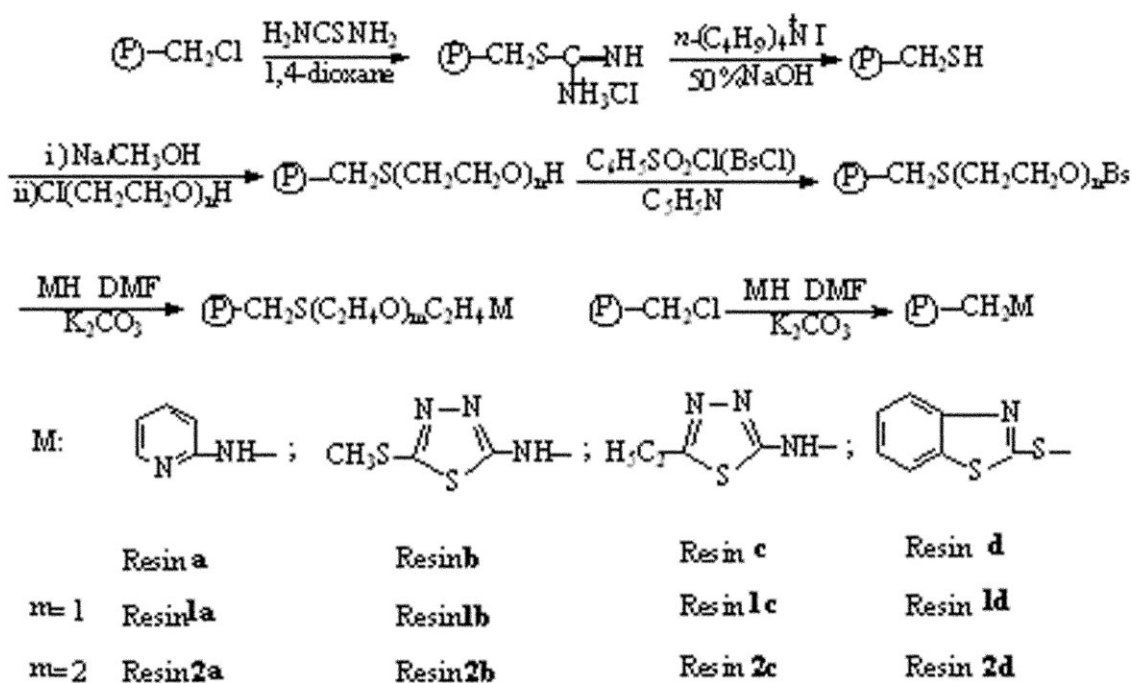
Scheme 1 Synthetic route to the resins.

solution adjusted to pH 3.0 and 1 mL of 0.1M Hg^{2+} solution. The mixture was shaken continuously at 25°C. At predetermined intervals, aliquots of 1 mL of solution were withdrawn, and the concentration of Hg^{2+} was determined by AAS.

Determination of K_d[22]

To determine the adsorption capacities of the resins toward Hg^{2+}, Ag$^+$, Cd^{2+}, and Pb^{2+}, they were put in contact with 5×10^{-3} M solutions of metal ions in 0.1M acetate buffer solution (pH 3.0). Thus, 30 mg of the resin was shaken with a mixture of 0.1M acetate buffer solution (19 mL) and 1 mL of 0.1M metal-ion solution at room temperature for 24 h. Then, the resin was separated by filtration, and the metal concentration in the solution was determined by AAS. The adsorption capacities were calculated according to eq. (1):

$$Q = \frac{(C_0 - C)V}{W} \qquad (1)$$

where Q is the adsorption amount (mmol/g); C_0 and C are the initial concentration and the concentration of metal ions in solution when the adsorbent is separated (mmol/mL), respectively; V is the volume (mL); and W is the dry weight of the resin (g).

K_d was calculated as the ratio of the amount of the metal ion sorbed by 1 g of the resin and the amount of metal ion left in 1 mL of the solution at equilibrium [shown as eq. (2)]:

$$K_d = \frac{Q}{C} \qquad (2)$$

where K_d is the distribution coefficient (mL/g), Q is the adsorption amount (mmol/g), and C is the concentration of metal ions in solution when the adsorbent is separated (mmol/mL).

RESULTS AND DISCUSSION

Characterization of resins a–d

Resins **a–d** were prepared according to the synthetic route shown in Scheme 1. The structures of resins **a–c** were characterized by the presence of new absorption peaks at 1384–1385 cm^{-1} corresponding to C—N stretching and by the absence of strong bands at 674 and 1265 cm^{-1} belonging to the C—Cl bond.[1] Furthermore, the formation of resins **a–c** was confirmed
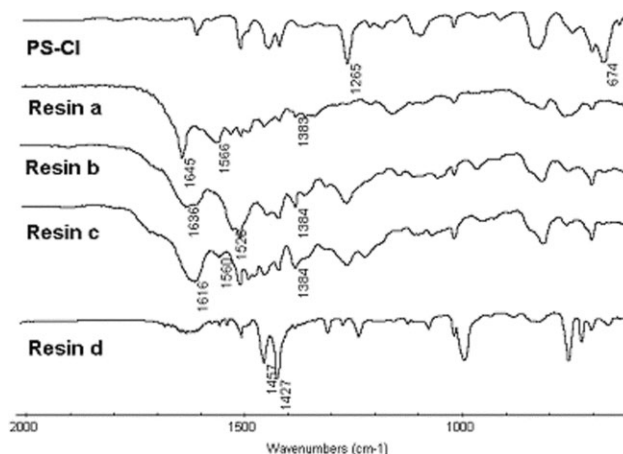

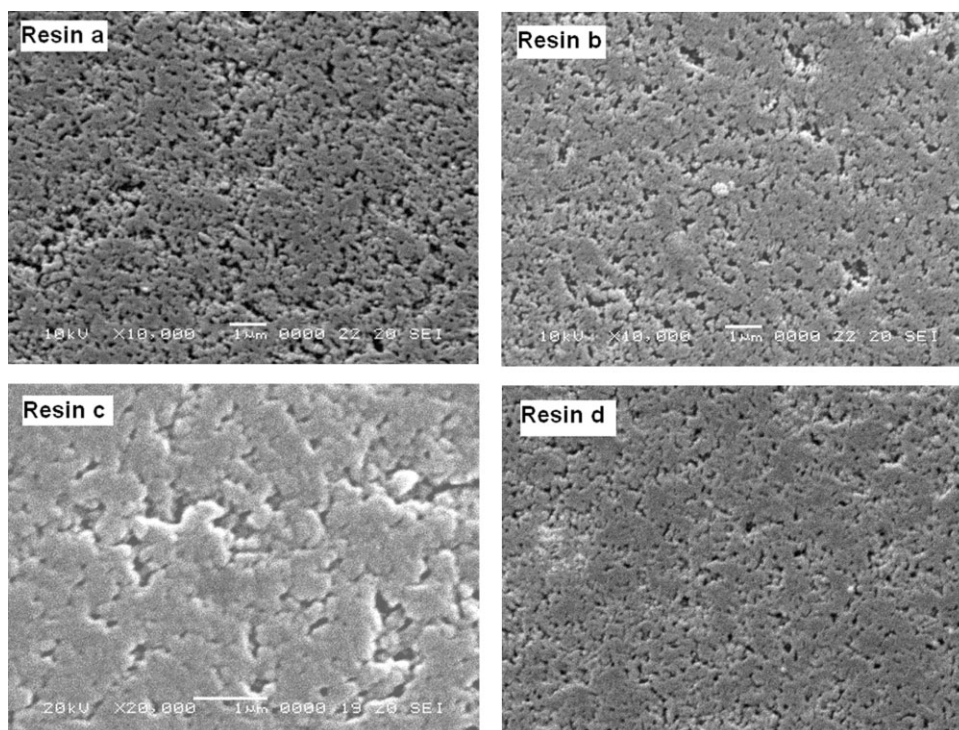**Figure 1** IR spectra of PS-Cl and resins **a–d**.

Figure 2 Scanning electron microscopy images of resins **a–d**.

by the presence of the characteristic bands of the corresponding heterocyclic functional groups, which indicated that the heterocyclic functional groups (AP, AETZ, and AMTZ) had been introduced into the polymeric matrix (see Fig. 1). In the case of resin **d,** its structure was confirmed by the disappearance of the characteristic peaks of the C—Cl bond and by the presence of strong bands at 1457 and 1427 cm^{-1} corresponding to the skeletal vibration of MBZ.[21] To observe the surface morphology of resins **a–d,** micrographs of the gold-coated samples were taken with a scanning electron microscope, and the images are shown in Figure 2. Obviously, there were abundant pores distributed on the surface of the resins

a–d, which indicated that the macroporous structure of PS-Cl had not been damaged after the reaction with the heterocyclic functional groups. The BET surface area and BJH desorption cumulative volume of the pores of resins **a–d** were determined and are listed in Table I.

Water absorption

The water absorption of the resins was determined, both with spacer arms and without them. These values are shown in Figure 3. From Figure 3, some conclusions could be drawn as follows: (1) for the resins
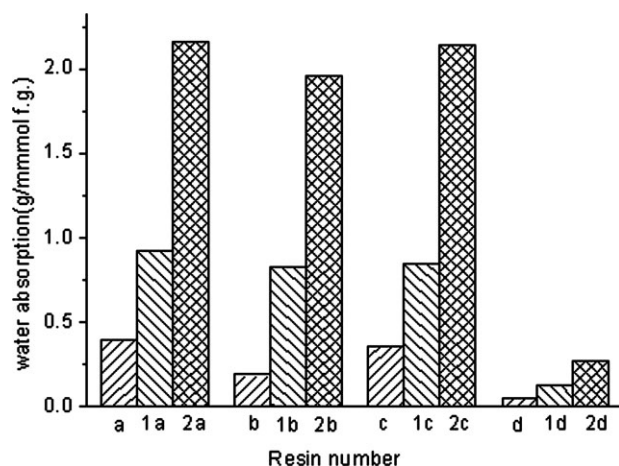

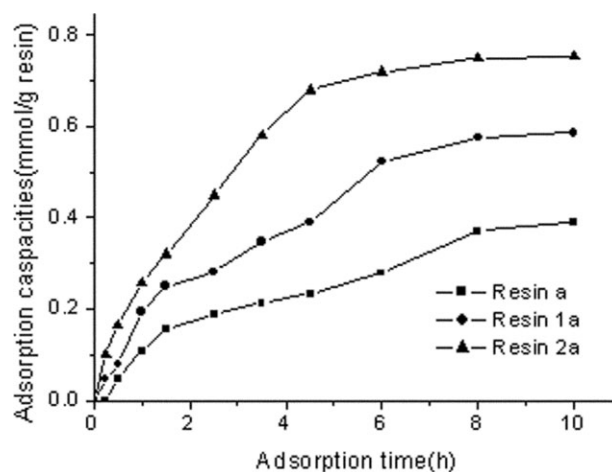**Figure 3** Water absorption of the resins.

Figure 4 Adsorption rates of resins **a**, **1a**, and **2a** for Hg^{2+} (25°C, pH = 3.0).
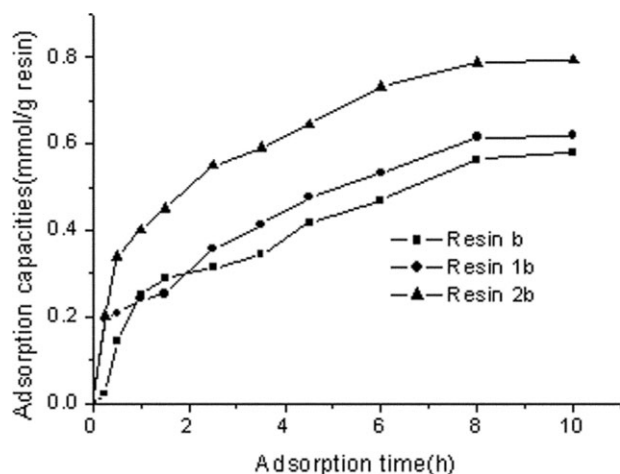
Figure 5 Adsorption rates of resins **b**, **1b**, and **2b** for Hg^{2+} (25°C, pH = 3.0).

without spacer arm, the order of the water absorption was Resin **a** > Resin **c** > Resin **b** > Resin **d**. This meant that, among the four heterocyclic rings, AP had the highest hydrophilicity, followed by AETZ, AMTZ, and MBZ. (2) For resins **a, 1a,** and **2a,** when a spacer arm was introduced between the heterocyclic functional group and the polymeric matrix, an increase in water adsorption was observed. The same experimental results were also found for the other series of resins. The increase in the water absorption could be ascribed to the presence of oxygen in the spacer arm, which could form hydrogen bonds with water. (3) As shown for resins **1a** and **2a,** the water absorption increased with increasing length of the spacer arms. Similar behavior was also observed for resins **1d** and **2d,** resins **1c** and **2c,** resins **1d** and **2d.** This showed that the increase in the length of the hydrophilic spacer arm was beneficial for improving the hydrophilicity of the polymeric matrix. All these aforementioned experimental data indicated that the
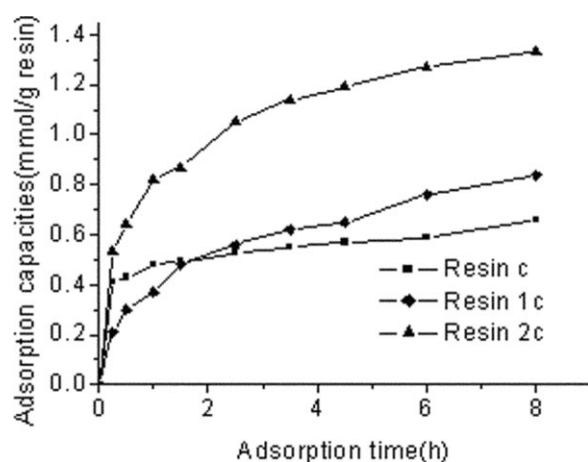
introduction of ethylene sulfide and ethylene oxide units as spacer arms could enhance the hydrophilicity of the polymer remarkably.

Adsorption kinetics of the resins

Because of the high adsorption capacity of the resins for Hg^{2+}, Hg^{2+} was chosen for investigating the adsorption kinetics (pH = 3.0). The adsorption rate curves of the resins for Hg^{2+} are shown in Figures 4–7. Figure 8 shows the results of the analysis of the data in Figure 4 with the Brykina equation:[23]

$$-\ln(1 - F) = kt \qquad (3)$$

where $F = Q_t/Q$ and Q_t and Q are the adsorption amounts at an adsorption time t and at equilibrium, respectively. The slope of the straight line made by the plotting of $-\ln(1 - F)$ versus t yielded the adsorption rate constant (k). By the analysis of the data in Figures 5–7 with the same method, the adsorption rate constants and correlation coefficients of the other resins were obtained and are listed in Table II.

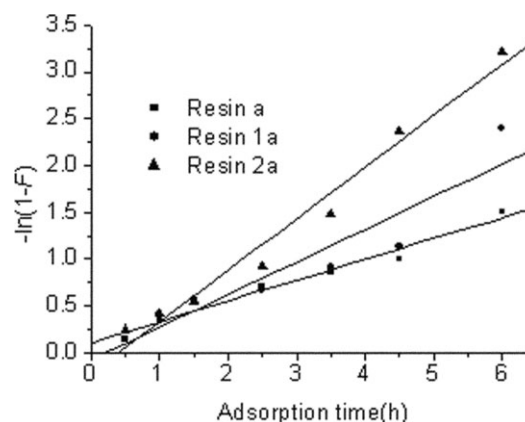**Figure 7** Adsorption rates of resins **d**, **1d**, and **2d** for Hg^{2+} (25°C, pH = 3.0).

Figure 6 Adsorption rates of resins **c**, **1c**, and **2c** for Hg^{2+} (25°C, pH = 3.0).

Figure 8 Relationship between $-\ln(1 - F)$ and t.

TABLE II
Adsorption Rate Constant (k) and
Correlation Coefficient (R^2)

Resin	k (10^{-5})	R^2
a	6.18	0.9828
1a	9.52	0.9589
2a	15.10	0.9870
b	6.75	0.9828
1b	7.87	0.9589
2b	11.20	0.9870
c	6.03	0.9898
1c	9.01	0.9859
2c	11.90	0.9969
d	5.60	0.9960
1d	7.17	0.9928
2d	10.20	0.9860

Figure 10 Adsorption capacities of the resins for Hg^{2+} at pHs 3 and 6.

As shown in Table II, (1) compared to the resins without spacer arm in the same series of resins, the ones with spacer arm had higher adsorption rate constants. (2) For the same series of resins (e.g., resin **a**, **1a**, and **2a**), the order of the adsorption rate constant was Resin **2a** > Resin **1a** > Resin **a**. The similar experimental results were also observed for the other series of resins. Obviously, the adsorption rate constants increased with increasing length of the spacer arm. All of the aforementioned experimental data implied that the introduction of a spacer arm produced an increase in the hydrophilicity of the functional group, which allowed for better contact between the metal ions in the aqueous solution and the chelating groups in the polymer, and increased the adsorption kinetic.

K_d values of the resins

To investigate the effect of the spacer arms on the adsorption capacity, metal ions, such as Hg^{2+}, Ag^+, Cd^{2+}, and Pb^{2+}, were chosen to determine the K_d
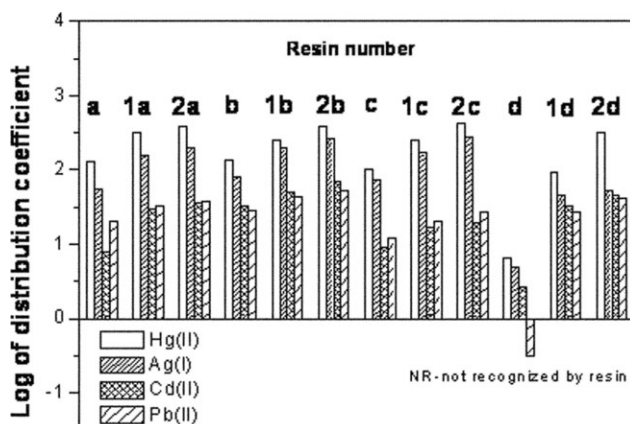
values of the resins at pH 3.0 under noncompetitive conditions. The values of log K_d obtained in these experiments are shown in Figure 9. From Figure 9, some conclusions were drawn, as follows:

1. The resins investigated in this study displayed high affinities toward Hg^{2+} and Ag^+, followed by Pb^{2+} and Cd^{2+}. This phenomenon could be attributed to the characteristic of the heterocyclic functional groups, which preferred interactions with large and more easily polarizable metal ions such as Hg^{2+} and Ag^+.[24]

On the basis of the adsorption behaviors of the resins for the aforementioned metal ions, Hg^{2+} and Ag^+ were chosen to investigate the effect of the pH value (3 and 6) on the adsorption capacities of the resins. The results are shown in Figures 10 and 11. As shown by these experimental data, the pH values of the metallic solutions had strong effect on the adsorption
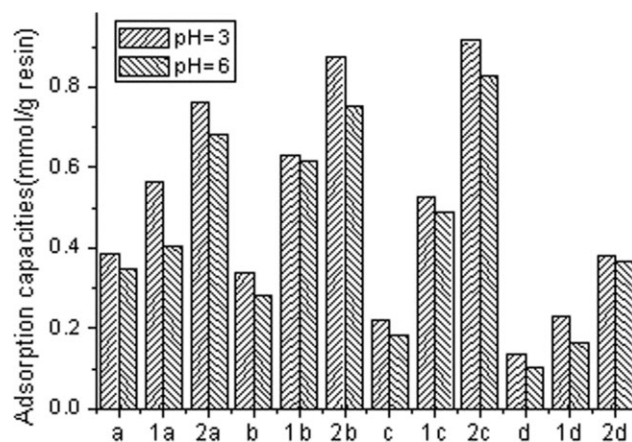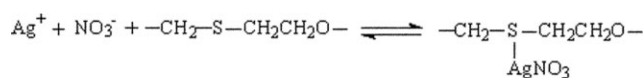

Figure 9 Log K_d of the resins for metal ions at pH 3.0.

Figure 11 Adsorption capacities of the resins for Ag^+ at pHs 3 and 6.

Scheme 2   Equilibrium equation between Ag$^+$, the S-coordinating atom, and the nitrate ion.

Scheme 3   Molecular model of resin 2a.

capacities of the resins for Hg^{2+} and Ag$^+$; that is, at lower pH, the adsorption capacities were higher than that at pH 6. This phenomenon was previously reported by Dong et al.[25] The reason might be the coordination bonding resulting from the S atom present in the spacer arms or in the heterocyclic functional groups of the resins. Because of the existence of the equilibrium equation (Ag$^+$ was chosen as the example; see Scheme 2) between Ag$^+$, the S atom, and the nitrate ion, the adsorption capacities of the resins for Ag$^+$ and Hg^{2+} increased with increasing the concentration of NO$_3^-$ in the metallic solution.

2. For resins a, 1a, and 2a, which contained the same kind of heterocyclic functional group (AP), one could note that resins 1a and 2a exhibited higher K_d values than resin a for all of the investigated metal ions. This phenomenon was also observed for other series of resins. These results indicate that the presence of the spacer arms between the polymeric matrix and the heterocyclic functional groups could increase the K_d values remarkably. The reason for the increase in K_d was the increase in hydrophilicity caused by the presence of the hydrophilic spacer arms, which allowed for better contact between the metal ion in solution and the functional group and increased the adsorption capacity.

In addition, as shown in Figure 9, for the same series of resins, such as resins 1a and 2a, the K_d values for the investigated metal ions increased with increasing length of the spacer arms. Similar experimental results were also observed between resins 1b and 2b, 1c and 2c, and 1d and 2d. A reasonable explanation for this was that the introduction of spacer arms might have increased the flexibility of the functional groups, which would have helped the functional group coordinate with the metal ions. To investigate the effect of the length of spacer arm on the flexibility of the functional groups, the stretched length of the chain and average end-to-end distance of the chain were calculated on an SGIO2 workstation according to the molecular model set up on the base of resin 2a (shown in Scheme 3). The results are shown in Table III. According to the theory of physical chemistry of macromolecules, the flexibility of the chain of a molecule can be characterized by the average end-to-end distance.[26] In general, the shorter the average end-to-end distance is, the more flexible the functional groups become. To eliminate the effect of the stretched length of the chain on the flexibility, we adopted the ratio of the average end-to-end distance to the stretched length of the chain to judge the flexibility of the functional groups. For each series of resins, the values of the stretched length of the chain increased with increasing length of the spacer arm, whereas the ratio of the average end-to-end distance to the stretched length of the chain decreased accordingly. These data indicated that the length of the spacer arm could have had an important effect on the flexibility of the functional

TABLE III
Ratio of the Average End-to-End Distance (h) to the Stretched Length of the Chain (l)

Resin	l (Å)	h (Å)	h/l	Adsorption capacity for Hg^{2+} (mmol/g)[a]
a	10.95	6.47	0.59	0.55
1a	19.50	8.77	0.45	1.07
2a	22.69	8.65	0.38	1.23
b	13.60	8.70	0.64	0.56
1b	22.12	12.06	0.55	0.92
2b	25.08	9.02	0.36	1.22
c	13.36	9.31	0.70	0.46
1c	21.88	11.96	0.55	0.95
2c	24.50	8.60	0.35	1.33
d	14.29	7.50	0.52	0.03
1d	22.33	9.17	0.41	0.40
2d	24.76	8.90	0.36	1.14

[a] The adsorption capacity was determined at pH 3.0.

groups. The increase in the flexibility of the functional group increased with the length of the spacer arm, which resulted in an increase in the K_d value.

3. As shown in Table III, the adsorption capacities of resins **1a–1c** and **2a–2c** toward Hg^{2+} were higher than their contents of functional groups, respectively. These experimental results indicate that the spacer arm containing heteroatoms such as oxygen and sulfur might have participated in the coordinating reaction of the metal ions,[19,20] which would have increased the adsorption capacities. For resins **1d** and **2d,** the aforementioned experimental phenomena were not observed. Their adsorption capacities were lower than the contents of their respective contents of functional groups. These results were attributed to the high hydrophobicity of MBZ, which made it difficult for resins **d, 1d,** and **2d** to swell sufficiently in aqueous solution; this thus resulted in a decrease in the adsorption capacities.

CONCLUSIONS

The adsorption properties, including water adsorption, adsorption kinetics, and adsorption capacities for metal ions, were tested for new chelating resins containing spacer arms and heterocyclic functional groups. This investigation showed that (1) the four kinds of heterocyclic functional groups showed high affinities for Hg^{2+} and Ag^+. (2) The presence of spacer arms between the heterocyclic functional group and the polymeric matrix evidently increased the hydrophilicity and improved the adsorption kinetics. (3) The presence of spacer arms in polymers might have increased the flexibility of chelating groups and participated in the coordination of metal ions, which resulted in an increase in the adsorption capacities for metal ions.

References

1. Chen, Y. Y.; Chen, X. W. J Macromol Sci Chem 1998, 25, 1443.
2. Wang, S. T.; Chen, W. Z.; He, B. L. Chem J Chin Univ 1987, 8, 81.
3. Nishide, H.; Shimidzu, N.; Tsuchida, E. J Appl Polym Sci 1982, 27, 4161.
4. Vernon, F.; Eceles, H. Anal Chim Acta 1973, 63, 403.
5. Willie, S. N.; Saturgeon, R. E.; Berman, S. S. Anal Chim Acta 1983, 149, 59.
6. Das, D.; Das, A. K.; Sinha, C. Talanta 1999, 48, 1013.
7. Pramanik, S.; Dhara, P. K.; Chattopadhyay, P. Talanta 2004, 63, 435.
8. Chattopadhyay, P.; Sinha, C.; Pal, D. K. Fresenius J Anal Chem 1997, 357, 368.
9. Chen, Y. Y.; Cai, G. P.; Wang, N. D. J Macromol Sci Chem 1990, 27, 1321.
10. Radi, S.; Ramdani, A.; Lekchiri, Y.; Morcellet, M.; Crini, G.; Morcellet, J.; Janus, L. Eur Polym J 2000, 36, 1885.
11. Qu, R. J.; Wang, C. H.; Sun, C. M.; Ji, C. N.; Cheng, G. X.; Wang, X. Q.; Xu, Q. J Appl Polym Sci 2004, 92, 1646.
12. Chwastowska, J.; Rogowska, A.; Sterlinska, E.; Dudek, J. Talanta 1999, 49, 837.
13. Sanchez, J. M.; Hidalgo, M.; Valiente, M.; Salvado, V. J Polym Sci Part A: Polym Chem 2000, 38, 269.
14. Sanchez, J. M.; Hidaigo, M.; Salvado, V. React Polym 2001, 46, 283.
15. Lezzi, A.; Cobianco, S.; Roggero, A. J Polym Sci Part A: Polym Chem 1994, 32, 1877.
16. Lezzi, A.; Cobianco, S. J Polym Sci Part A: Polym Chem 1994, 54, 889.
17. Bourdeland, J. L.; Campa, C.; Font, J.; de March, P. Eur Polym J 1989, 25, 197.
18. Cobianco, S.; Lezzi, A.; Scotti, R. React Polym 2000, 43, 7.
19. Lauth, M.; Frere, Y.; Meurer, B.; Gramain, P. H. React Polym 1990, 12, 155.
20. Lauth, M.; Frere, Y.; Prevost, M.; Gramain, P. H. React Polym 1990, 13, 73.
21. Ji, C. N.; Qu, R. J.; Sun, C. M.; Wang, C. H.; Xu, Q.; Sun, Y. Z.; Li, C. X.; Guo, S. H. J Appl Polym Sci 2007, 103, 3220.
22. Andrzej, W. T.; Bozena, N. K. Eur Polym J 2000, 36, 2359.
23. Brydkina, G. D.; Marchak, T. V.; Krysina, L. S.; Belyavskaya, T. A. Zh Anal Khim 1980, 35, 2294.
24. Pearson, R. G. J Am Chem Soc 1963, 25, 3533.
25. Dong, S. H.; Tang, W. X.; Hu, Y. H. Acta Polym Sinica 1990, 2, 142.
26. He, M. J.; Chen, W. X., Dong, X. X. Physics of Macromolecule; Fudan: Shanghai, 2000; p 20.